Journal of Applied Polymer Science

Structure, mechanical, and electrical properties of high-density polyethylene/multi-walled carbon nanotube composites processed by compression molding and blown film extrusion

Dong Xiang,[1] Eileen Harkin-Jones,[2] David Linton,[3] Peter Martin[1]

[1]School of Mechanical and Aerospace Engineering, Queen's University Belfast, BT9 5AH, United Kingdom
[2]School of Engineering, University of Ulster, BT37 0QB, United Kingdom
[3]School of Electronics, Electrical Engineering, and Computer Science, Queen's University Belfast, BT9 5BN, United Kingdom
Correspondence to: E. Harkin-Jones (E-mail: e.harkin-jones@ulster.ac.uk) and D. Xiang (E-mail: dxiang01@qub.ac.uk)

ABSTRACT: The structure and properties of melt mixed high-density polyethylene/multi-walled carbon nanotube (HDPE/MWCNT) composites processed by compression molding and blown film extrusion were investigated to assess the influence of processing route on properties. The addition of MWCNTs leads to a more elastic response during deformations that result in a more uniform thickness distribution in the blown films. Blown film composites exhibit better mechanical properties due to the enhanced orientation and disentanglement of MWCNTs. At a blow up ratio (BUR) of 3 the breaking strength and elongation in the machine direction of the film with 4 wt % MWCNTs are 239% and 1054% higher than those of compression molded (CM) samples. Resistivity of the composite films increases significantly with increasing BURs due to the destruction of conductive pathways. These pathways can be recovered partially using an appropriate annealing process. At 8 wt % MWCNTs, there is a sufficient density of nanotubes to maintain a robust network even at high BURs. © 2015 Wiley Periodicals, Inc. J. Appl. Polym. Sci. **2015**, *132*, 42665.

KEYWORDS: composites; films; graphene and fullerenes; manufacturing; nanotubes; properties and characterization

Received 5 May 2015; accepted 25 June 2015
DOI: 10.1002/app.42665

INTRODUCTION

Carbon nanotubes (CNTs) have exhibited great potential for the fabrication of multifunctional polymer based composites due to their low density and unique mechanical, electrical, and thermal properties.[1,2] They are increasingly finding applications in aerospace and automotive industries for antistatic, electrostatic dissipation (ESD), and electromagnetic interference (EMI) shielding when light weight, flexibility, and low cost are required. However, the theoretical reinforcements in some of these properties have not been achieved due to the presence of CNT aggregates as a result of the strong van der Waals forces between nanotubes. The method of preparation of the nanocomposites can have a very significant effect on the dispersion of nanotubes in the matrix polymer. There are three main methods of preparing polymer/CNT composites: in-situ polymerization,[3] solution mixing,[4] and melt mixing.[5–9] Although in-situ polymerization and solution mixing can provide improved dispersion of nanotubes, melt mixing is a simpler and more effective method, particularly from an industrial perspective and it is the route that is of interest to the authors of this article. Previous studies of the melt mixing process of polymer/CNT composites have been reported[7,10–12] where it was found that the distribution and dispersion of CNTs are dependent on many factors such as the polymer viscosity, residence time, screw speed, and screw configuration, etc.

In different polymer processing operations, the polymer/CNT composites will experience different deformational and thermal regimes and this is likely to result in different structure, and hence properties, in the final products. For example, in injection molding, the deformation will be mainly by shear while in blown film extrusion the deformation will be mainly elongational. In much of the published research to date on polymer/CNT composites, compression molding has been employed to prepare sample specimens for structural and property characterization studies.[10,11,13,14] Kasaliwal *et al.*[15] investigated the effect of compression molding temperature and time on the electrical volume resistivity of polycarbonate (PC)/multi-walled carbon nanotube (MWCNT) composites near the percolation threshold (1 wt %). It was observed that the resistivity decreased with increasing molding temperature or molding time due to the presence of more nanotube secondary agglomeration, which enhanced conductive pathways. Similar results were also shown in Yu's study[16] of the surface resistivity of ethylene-vinyl acetate

(EVA) copolymer/MWCNT composites. In Choong's study[17] of polycarbonate (PC)/MWCNT composites processed by compression molding and injection molding, it was observed that the mechanical and electrical properties of the composites were affected by the processing history. Although several billion pounds of polymers are processed into films by blown film extrusion technique every year[18] and the blown film extrusion process of pure polymers has been investigated in some previous articles,[19–21] there are very few studies of the blown film extrusion of polymer/CNT composites. Russo *et al.*[22] prepared thermoplastic polyurethane (TPU)/multi-walled (MWCNT) thin composite films using blown film extrusion and chill-roll or cast film extrusion. In their study, it was observed that chill-roll extrusion can achieve a better CNT dispersion compared to blown film extrusion at the same loading and extrusion temperatures. Tensile testing showed that the blown films exhibited lower elastic modulus and higher elongation at break compared to the cast films. However, the electrical properties of the blown and cast films were not investigated in their study. In this study, we are interested in examining the differences in structure and properties that arise due to two processes of interest (1) compression molding because it is the main method to produce samples for laboratory studies of nanocomposites and (2) blown film extrusion because it is a major commercial method to produce thin plastic films that are used in areas such as packaging. A previous study[23] by one of the authors demonstrated substantial differences in structure and properties of high-density polyethylene (HDPE)/nanoclay composites made via different processing routes.

In this current study, melt mixed HDPE/MWCNT composites prepared by two different processing routes will be examined to determine if similar differences arise due to processing route as did with the HDPE/nanoclay composites. This study will be significant to better realize the effect of different processing routes on the structure and properties of polymer/CNT composites. To the best of author's knowledge, there has been no publication on the blown film extrusion of HDPE/CNT composites yet, although HDPE is a very important commercial polymer.

EXPERIMENTAL

Materials

High-density polyethylene, grade HDPE HTA-108, in pellet form was obtained from ExxonMobil. It has an average molecular weight of 123,400 g/mol and a density of 0.961 g/cm^3. This high molecular weight is necessary to enable the material to be blown into a film via the blown film extrusion process. The melt flow index (MFI) of the HDPE is 0.7 g/10 min. The multi-walled carbon nanotubes (NC7000) with a purity of 90% were kindly supplied by Nanocyl SA, Belgium. The nanotubes have a nominal diameter of 9.5 nm and a nominal average length of 1.5 μm.[5] The density of the MWCNTs is 1.85 g/cm^3.[24]

Composite Preparation

The HDPE pellets were ground, at room temperature, into a powder using a Wedco SE-12 UR pilot plant grinder operating at 7000 rpm and with a gap size set to 400 μm. The HDPE powder was premixed for 2 min with the MWCNTs at a speed of 2000 rpm/min using a PRISM Pilot 3 high-speed mixer. The blends, containing 2, 4, and 8 wt % MWCNT loadings, were melt mixed in a Collin co-rotating twin-screw extruder ZK 25 with a temperature profile of 175, 220, 220, 215, 210, and 200°C from zones 1 to 6. An additional mixing element was used to produce a more intensive mixing and a reverse conveying element after the mixing zone was used to increase mixing time. In Mayoral's study at Queen's University Belfast,[12] it was observed that this screw profile was very effective in dispersing MWCNTs in poly(propylene) and resulted in conductive composites. The screw speed was set at 150 rpm. The residence time of melt in the extruder barrel is 1.5 min. The extruded strand was cooled in a water bath and pelletized.

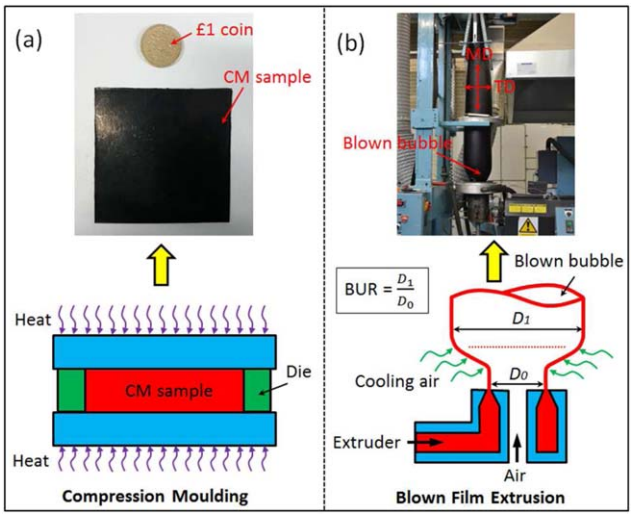

Figure 1. Schematic diagram of the compression molding (a) and blown film extrusion (b) of the HDPE/MWCNT composites. [Color figure can be viewed in the online issue, which is available at wileyonlinelibrary.com.]

Processing

The extruded pellets were compression molded (CM) in a steel mold of 1 mm thickness at 200°C and 100 bars for 5 min followed by a slow cooling at approximate 20°C/min using a Collin P200P platen press machine in order to produce sheet samples.

Blown film extrusion of the pure HDPE and HDPE/MWCNT composite pellets with 2, 4, and 8 wt % MWCNTs was conducted using a 38 mm Killion single-screw extruder equipped with a film blowing die (outer diameter 75 mm, annular gap 1 mm) and cooling tower. The barrel temperature from zone 1 to 8 was 190, 230, 230, 230, 250, 250, 250, and 250°C, respectively. The screw speed was 35.6 rpm, and the take-up rate was 6.9 m/min. The pressure in the barrel was measured using an inline pressure gauge. The materials were blown into films with blow up ratios (BURs) of 2, 2.5, and 3. BUR is the ratio of the bubble diameter (D_1) D_1 to the die diameter (D_0 D_0). The average thickness of blown films was obtained by measuring the thickness at 10 points distributed evenly along the film circumference using a Mitutoyo 293–821 micrometer with a resolution of 1 μm. Figure 1 shows a schematic diagram of the compression molding and blown film extrusion of the HDPE/MWCNT composites.

Table I. Annealing Parameters Used for Blown Films Containing 4 wt % MWCNTs

BUR	Annealing temperature (°C)	Annealing time (h)
2	130	0.5, 2, and 4
2	140	0.5, 1, and 2
3	140	0.5, 1, and 2
3	150	0.5, 1, and 2

Annealing of the blown films of HDPE/MWCNT composites with 4 wt % MWCNTs was carried out in an oven in order to study the influence of annealing on the electrical properties of the films. The samples for annealing were glued to an aluminum plate to prevent shrinkage and distortion of the sample. The detailed annealing parameters are shown in Table I.

Characterization

Oscillatory Rheology. An AR-G2 oscillatory rheometer with parallel plate geometry (Standard ETC steel plate, 25 mm diameter, 1 mm gap) was used to analyze the viscosity variation of the composites. Circular specimens (diameter 25 mm, thickness 1 mm) were cut from the compression molded sheets. Tests were performed at a temperature of 200°C. All measurements were taken in the linear viscoelastic region (strain 1%) measured by strain sweeps, in which the storage modulus and loss modulus were independent of strain amplitude. Dynamic frequency sweeps were then conducted in the linear viscoelastic region with sweep frequency varied from 0.1 to 100 rad/s.

Scanning Electron Microscopy (SEM). The morphology of MWCNTs in the compression molded sheets and blown films was investigated using a JEOL 6500F SEM with an operating voltage of 5.0 kV. All samples for SEM analysis were plasma etched for 60 s at an etching power of 100 W using a reactive ion etching system (STS Cluster C005). Then the etched samples were gold sputtered prior to imaging.

Differential Scanning Calorimetry (DSC). A Perkin-Elmer DSC model 6 was used to measure the percentage crystallinity, melting, and crystallization behavior of the materials under an inert nitrogen atmosphere. Samples with a mass of 7∼10 mg were cut from the compression molded sheets and blown films. The samples were heated from 30°C to 200°C at a heating rate of 10°C/min, held at 200°C for 3 min, followed by a cooling process from 200°C to 30°C at a cooling rate of 10°C/min. The samples were then reheated to 200°C again at 10°C/min. Three repeated tests were conducted for each sample. DSC was also used to estimate the crystallinity of blown films during the annealing process. A sample cut from the blown film, with a typical mass of 7∼10 mg, was heated rapidly in the DSC from room temperature to 130°C at a heating rate of approximately 300°C/min, then held for 5 min under an isothermal condition. Subsequently, the sample was heated to around 170°C at a rate of 10°C/min to see whether a melting peak would occur.

In this study, the heat of fusion of 100% HDPE crystal (ΔH_m°) was taken as 293 J/g,[25] and then the degree of crystallinity (Xc) was calculated using eq. (1):

$$Xc = \frac{\Delta H_m}{(1 - M_{CNT})\Delta H_m^\circ} \times 100\% \quad (1)$$

where ΔH_m is the enthalpy of fusion of sample (J/g); M_{CNT} is the weight fraction of MWCNTs.

Tensile Testing. Tensile tests were conducted for the compression molded sheets and blown films using an Instron 5564 Universal Tester at room temperature (BS EN ISO 527:1996). Young's modulus was determined using a clip-on extensometer at a crosshead speed of 5 mm/min. Stress at break and elongation values were taken at a crosshead speed of 50 mm/min to improve the efficiency of tests.[26–28] Five samples were tested for each sheet and average values were calculated.

Electrical Resistivity Testing. Volume resistivity testing was carried out for the compression molded sheets and blown films. For the samples with a high resistivity ($>10^8$ Ω), volume resistivity testing was performed using a Keithley 6517A high resistivity electrometer equipped with a Keithley 8009 resistivity test fixture according to ASTM-D257. In this method, the circular samples cut from the compression molded and blown films have a diameter of 70 mm. For more conductive samples ($\leq 10^8$ Ω), two-point probe measurements were conducted using a Keithley DMM2000 multimeter. The strips with dimensions of 50 mm × 10 mm were cut from the compression molded and blown films. Silver paste was used to minimize contact resistance effects in the two-point probe measurements. Two specimens for each type were tested.

RESULTS AND DISCUSSION

Effect of MWCNTs on Rheological Behavior

Oscillatory rheology testing was conducted to investigate the effect of the addition of MWCNTs on the rheological properties of the HDPE matrix. The complex viscosity (η^*) and storage modulus (G') of the pure HDPE and HDPE/MWCNT composites measured at 200°C as a function of sweep frequency are shown in Figure 2(a,b), respectively. It can be observed that the complex viscosity of the pure HDPE and composites decreases steadily with increasing shear rates, indicating a typical non-Newtonian behavior in the frequency range. The addition of MWCNTs to the polymer matrix clearly leads to increases in both complex viscosity and storage modulus of the material. For a highly dispersed and distributed filler in a polymer matrix, a sudden increase in complex viscosity η^* and storage modulus G' at low frequencies is representative of a transition from liquid-like to solid-like (or pseudo-solid-like) viscoelastic behavior. These changes are expected from the formation of a percolated network-like structure due to the interactions between the MWCNTs and the polymer matrix.[7,14] In this case, the transition from liquid-like to solid-like can be seen at 2 wt % MWCNTs, where the η^* and G' increased by over 180% and 330%, respectively, compared to the pure HDPE at the frequency of 0.1 rad/s. The onset of the rheological percolation threshold may be more clearly identified from Cole–Cole plot (plot of storage modulus G' versus loss modulus G''), and any deviation from a linear relationship between G' and G'' reflects the formation of a rheological percolation network.[8] Figure 2(c) shows the Cole–Cole plot, from which one can see that the G'

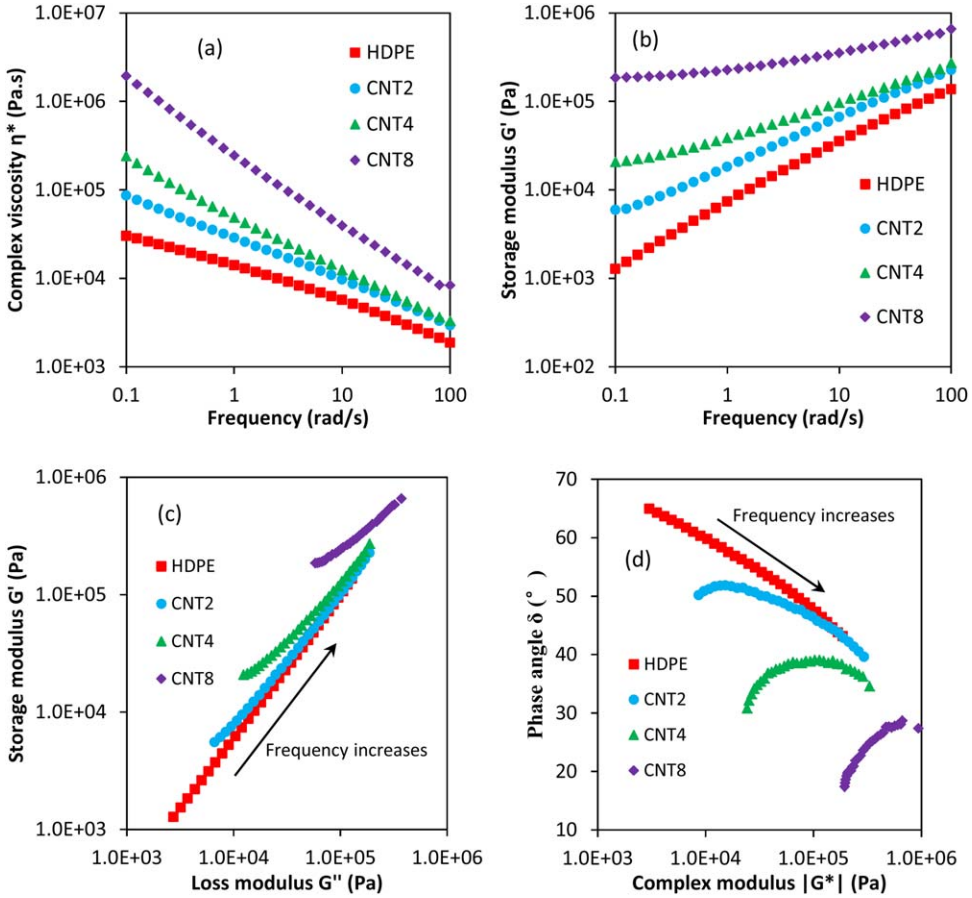

Figure 2. Variations of complex viscosity (a) and storage modulus (b) with frequency, Cole–Cole plot (c) and van Gurp-Palmen plot (d) for the HDPE/MWCNT composites. [Color figure can be viewed in the online issue, which is available at wileyonlinelibrary.com.]

and G'' of the pure HDPE always remain a linear relationship while a deviation from the linear relationship occurs with the inclusion of 2 wt % MWCNTs. In addition, a van Gurp-Palmen plot (plot of phase angle δ versus complex modulus $|G^*|$) is also used to examine the structural changes in the systems [Figure 2(d)], which can very sensitively reflect the formation of network-like structures in nanofiller reinforced polymer composites. In the van Gurp-Palmen plot, the rheological percolation threshold is determined at a certain (critical) concentration where the phase angle clearly decreases with decreasing complex modulus.[29] In Figure 2(d), a remarkable shift in the shape of the curve can be observed with the addition of 2 wt % MWCNTs compared to the curve for pure HDPE, and an evident decrease in δ in the curve for the HDPE/MWCNT composite containing 2 wt % MWCNTs occurs with decreasing complex modulus. Therefore, solid-like behavior can be confirmed at the MWCNT loading of 2 wt %, while the rheological percolation threshold for the HDPE/MWCNT composites would be at a slightly lower MWCNT loading. Furthermore, one can see from the rheological results shown in Figure 2 that the network-like structures in the systems are enhanced steadily with increasing MWCNT content, which will certainly have an impact on the processing of the HDPE/MWCNT composites. The network-like structures are also observed in the SEM results [Figure 5(a–c)].

Blown Film Extrusion

Blown film extrusion of the pure HDPE and HDPE/MWCNT composite pellets with 2, 4, and 8 wt % MWCNTs was carried out at BURs of 2, 2.5, and 3. The rheological behavior of the composites has been discussed earlier. Figure 3 shows the complex viscosity of various blends of HDPE/MWCNT (at a sweep

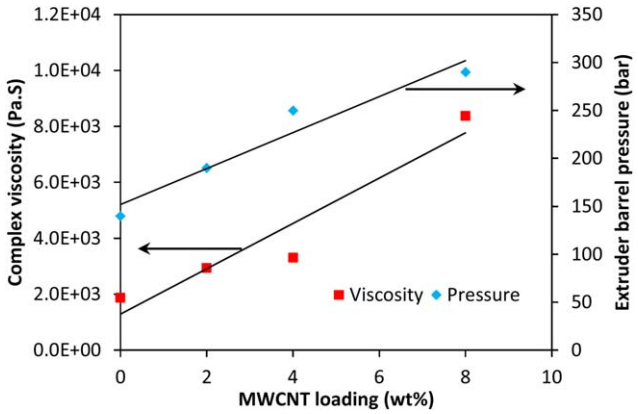

Figure 3. Complex viscosity (at a frequency of 100 rad/s and temperature of 200°C) and extruder barrel pressure as a function of MWCNT loadings. [Color figure can be viewed in the online issue, which is available at wileyonlinelibrary.com.]

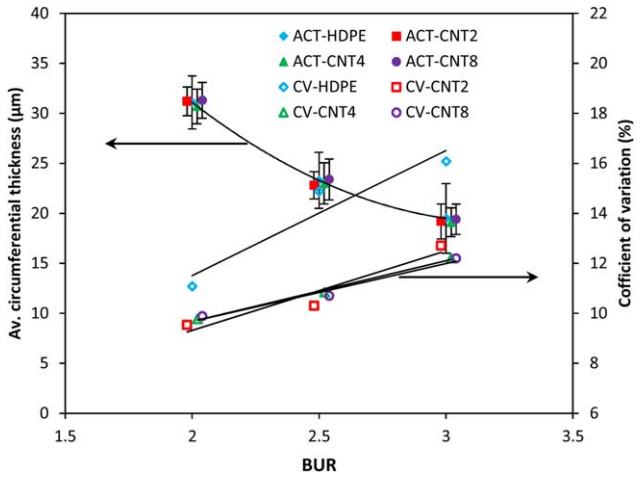

Figure 4. Average circumferential thickness of the blown films and the coefficients of variation for the circumferential thickness with increasing BURs. [Color figure can be viewed in the online issue, which is available at wileyonlinelibrary.com.]

frequency of 100 rad/s, which is similar to extrusion conditions and a temperature of 200°C) plotted alongside the extruder barrel pressure recorded during blown film extrusion as a function of MWCNT loadings. It can be observed that the pressure in the barrel increases with increasing MWCNT content, which can be attributed to the increased viscosity of the melt with the addition of MWCNTs. There is a doubling of pressure in going from an unfilled HDPE up to one with a content of 8 wt % MWCNTs. This has significant implications for both equipment capability and energy consumption in processing.

The average circumferential thickness (ACT) of the blown films with increasing BURs was measured and is shown in Figure 4. The coefficients of variation (CV), the ratio of the standard deviation to the corresponding average circumferential thickness, for the ACT of thin films were calculated and are also shown in Figure 4. The data points are horizontally offset for clarity. It can be seen in Figure 4 that the ACT of the thin films of both pure HDPE and HDPE/MWCNT composites nonlinearly decreases from around 30 to 20 μm with increasing BUR. The inclusion of MWCNTs does not influence the ACT of the thin films under the same processing conditions. The CVs increase for both pure HDPE and the composite films with increasing BURs. However, the CVs for the composite thin films appear to be smaller compared with the pure HDPE. This is most likely to be due to the biaxial deformation of the material during film blowing being more stable with the addition of MWCNTs. In authors' previous study of biaxial stretching of the HDPE/MWCNT composites,[13,30] it was found that the HDPE/MWCNT composites exhibit a stronger strain hardening behavior during biaxial deformation compared to pure HDPE, which contributes to a more uniform thickness distribution of the deformed samples.

Morphology

The morphology of MWCNTs in the compression molded sheets and blown films were investigated using SEM, as shown in Figure 5. Figure 5(a–c) show the SEM images for the compression molded composites with 2, 4, and 8 wt % MWCNTs, respectively, in which the MWCNTs are randomly oriented and a network-like structure of nanotubes can be observed. The individual nanotubes and secondary agglomerates, which can enhance the formation of conductive networks[10] are homogeneously distributed in the polymer matrix. The SEM images for the blown films of HDPE/MWCNT composite containing 4 wt % MWCNTs at BURs of 2 and 3 are shown in Figure 5(d,e), respectively. In Figure 5(d), MWCNTs oriented along the flow direction and randomly oriented can be observed at a BUR of 2. Figure 5(e) shows that there is less clear MWCNT orientation along the machine direction (MD) and fewer MWCNT agglomerates due to the increased deformation in the transverse direction (TD) at a BUR of 3. The morphology of the blown composite film was also investigated after annealing. It is clear that the disentangled MWCNTs in the blown film containing 4 wt % MWCNTs at a BUR of 3 have reagglomerated after the annealing process as shown in Figure 5(f). The reagglomeration of nanotubes in polymers after an annealing process was also observed by Alig[31] and Jiang.[32]

DSC

The melting and crystallization behaviors of the compression molded sheets and blown films (BURs = 2 and 3) of pure HDPE and HDPE/MWCNT composites containing 4 and 8 wt % MWCNTs were investigated using DSC. Some additional structural information can be revealed from the thermal behavior of the processed samples in the heating and crystallization stages, particularly the first heating stages.[13] The crystallinities from DSC tests are calculated according to the fusion enthalpies during the first and second melting stages, respectively. Figure 6(a–c) show the thermograms of the samples in the first heating stage, and Figure 6(d) shows some typical thermograms in the cooling stage. The detailed thermal parameters are presented in Table II.

It can be observed in Figure 6(a–c) that the melting peaks of the blown films of pure HDPE and HDPE/MWCNT composites shift to a slightly lower temperature relative to the corresponding compression molded samples. This can be attributed to a decreased crystallite size resulting from incomplete crystallization during the rapid cooling process in blown film extrusion.[33,34] Table II shows that the melting temperature in the first heating stage (T_m^{1st}) of the blown films at BURs of 2 and 3 decreases by about 1∼2°C. It can be seen in Table II that the addition of MWCNTs does not influence the crystallinity in the first heating stage (X_c^{1st}) for all the compression molded samples. The X_c^{1st} of the blown films of pure HDPE does not change compared with the compression molded sample (all the values of crystallinity are ∼70%) though a strain induced crystallization might be expected in the blown film, while that of HDPE/MWCNT composites exhibits a slight increase of about 5% after blown film extrusion, as shown in Table II. This increase in X_c^{1st} for the blown composite films may be due to a more efficient heterogeneous nucleation influence of MWCNTs[35] that occurs in the blown film due to disentanglement of CNTs under elongational deformation. The nucleation effect of MWCNTs can be observed in the cooling stage of the DSC tests, where the crystallization temperature (T_c) of all the

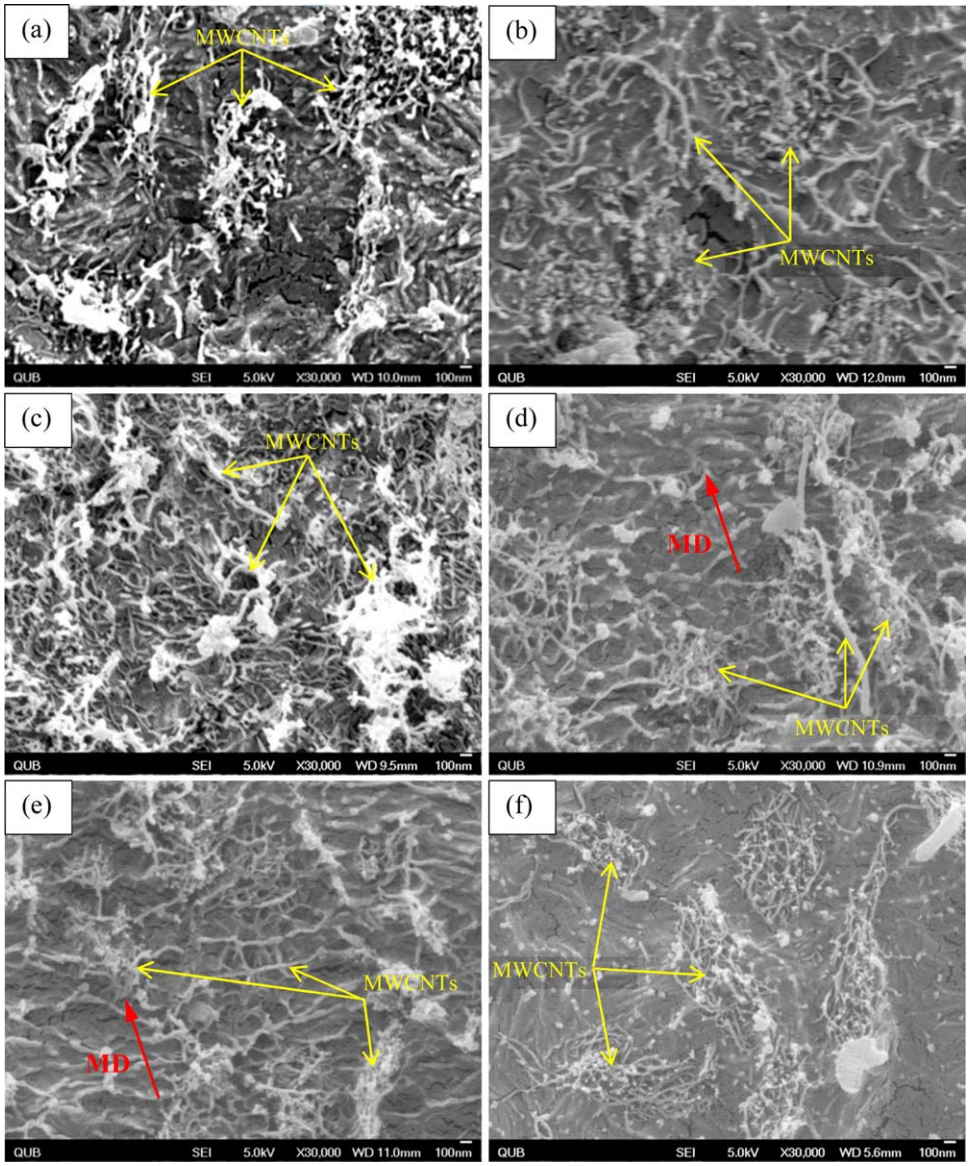

Figure 5. SEM images: (a–c) the compression molded composites containing 2, 4, and 8 wt % MWCNTs, respectively; (d–e) the blown films containing 4 wt % MWCNTs with BURs of 2 and 3, respectively; and (f) the annealed blown film containing 4 wt % MWCNTs with a BUR of 3 at 140°C for 2 h. [Color figure can be viewed in the online issue, which is available at wileyonlinelibrary.com.]

composites with 4 and 8 wt % MWCNTs increases by approximate 2°C compared to pure HDPE (Table II). It can be seen in Figure 6(d) that the crystallization behavior of the filled and unfilled samples is not influenced substantially by the processing routes in this study. The decreased width at half height in the first heating curves (W_h^{1st}) of the blown films indicates a narrower distribution of crystallite sizes relative to the compression molded samples[36] as would be expected due to more rapid cooling and more efficient nucleation efficiency of disentangled nanotubes. Interestingly, the crystallinity in the second heating stage (X_c^{2nd}) of the blown films containing 4 and 8 wt % MWCNTs is still ~5% higher than that of all the pure HDPE samples and compression molded composite sheets, although the thermal history of the samples has been removed in the first heating stage. This can be attributed to the increased nucleation sites in the HDPE/MWCNT composites due to disentanglement of MWCNTs during blown film extrusion. There is no significant difference in the melting temperature in the second heating stage (T_m^{2nd}) for all the compression molded sheets and blown films due to the removal of thermal history. The T_m^{2nd} of all the blown films increases by about 2°C compared to their T_m^{1st}, as shown in Table II.

Tensile Testing

Tensile testing was conducted to investigate the mechanical properties of the compression molded sheets and blown films. First of all, the effect of the addition of MWCNTs on the tensile properties of all the compression molded sheets was characterized, as shown in Figure 7. It can be seen in Figure 7(a) that the Young's modulus (E) is steadily improved by the presence

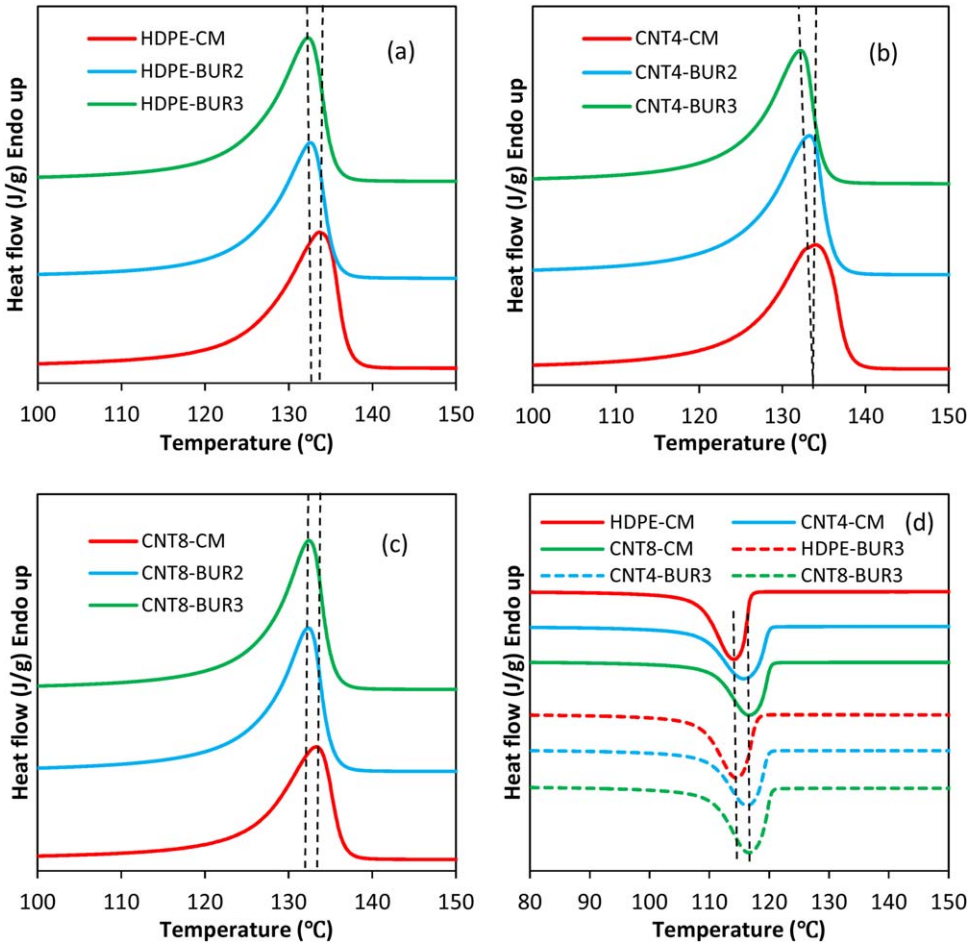

Figure 6. DSC thermograms of the compression molded samples and blown films of pure HDPE and HDPE/MWCNT composites with different BURs in the first heating (a–c) and cooling (d) stages. [Color figure can be viewed in the online issue, which is available at wileyonlinelibrary.com.]

of MWCNTs. The modulus of compression molded composites with 2, 4, and 8 wt % MWCNTs significantly increases by 42%, 112%, and 163%, respectively (Table III). The experimental modulus is compared with the theoretical values from a Halpin-Tsai composite model. According to the Halpin-Tsai model,[37–40] the longitudinal (E_{11}) and transverse (E_{22}) modulus can be predicted using eqs. (2) and (3), respectively. However, for the compression molded composite sheets in which the MWCNTs are randomly oriented, the Halpin-Tsai model can be expressed as eq. (4). It can be observed in Figure 7(a) that the predicted Young's modulus (Modulus-E_r) for the compression molded composites using eq. (4) agrees very well with the experimental results (Modulus-E_x) at low MWCNT loadings ($\leq$ 4 wt %). The predicted value is 21% higher than the experimental one at a MWCNT loading of 8 wt % due to the presence of more nanotube agglomerates.

Table II. Thermal Parameters of the Compression Molded Samples and Blown Films of Pure HDPE and HDPE/MWCNT Composites with Different BURs

Sample	X_c^{1st} (%)	T_m^{1st} (°C)	W_h^{1st} (°C)	T_c (°C)	X_c^{2nd} (%)	T_m^{2nd} (°C)
HDPE-CM	72.8 ± 3.1	133.9 ± 0.2	7.4 ± 0.1	114.0 ± 0.2	70.4 ± 1.3	134.1 ± 0.1
CNT4-CM	73.9 ± 5.1	134.0 ± 0.1	7.7 ± 0.3	116.0 ± 0.2	70.7 ± 2.4	134.3 ± 0.2
CNT8-CM	70.9 ± 3.5	133.6 ± 0.3	7.1 ± 0.3	116.2 ± 0.4	72.6 ± 1.9	133.9 ± 0.4
HDPE-BUR2	72.3 ± 2.9	132.8 ± 0.2	6.6 ± 0.2	114.2 ± 0.2	70.1 ± 2.5	134.5 ± 0.2
HDPE-BUR3	73.7 ± 1.4	132.4 ± 0.1	6.6 ± 0.1	114.2 ± 0.4	71.5 ± 1.3	134.5 ± 0.1
CNT4-BUR2	76.6 ± 3.6	133.0 ± 0.7	6.8 ± 0.1	115.5 ± 0.4	75.2 ± 3.0	135.3 ± 0.1
CNT4-BUR3	77.2 ± 3.0	132.3 ± 0.2	6.6 ± 0.4	116.0 ± 0.3	74.7 ± 1.1	134.7 ± 0.5
CNT8-BUR2	76.6 ± 1.5	132.4 ± 0.2	5.7 ± 0.3	116.3 ± 0.1	75.1 ± 2.7	134.0 ± 0.2
CNT8-BUR3	76.6 ± 1.4	132.6 ± 0.2	5.9 ± 0.2	116.5 ± 0.2	75.8 ± 2.8	134.9 ± 0.2

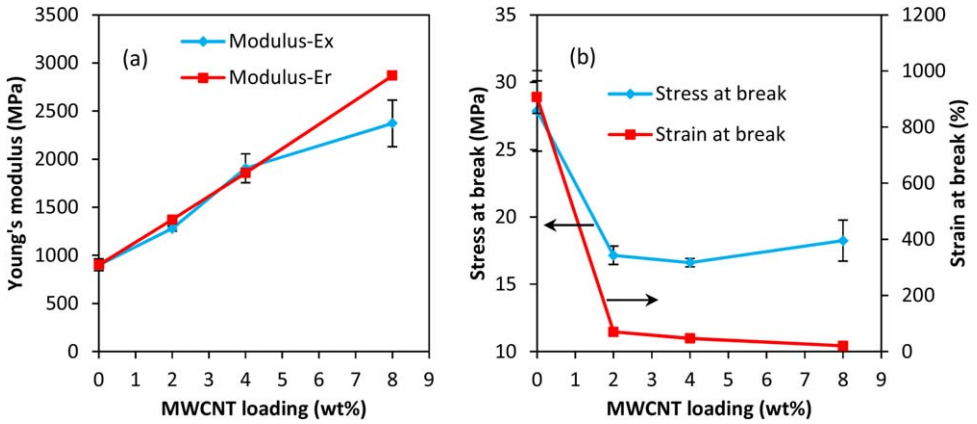

Figure 7. Experimental and predicted Young's modulus (a) and stress at break and strain at break (b) of the compression molded HDPE/MWCNT composites. [Color figure can be viewed in the online issue, which is available at wileyonlinelibrary.com.]

$$\frac{E_{11}}{E_m}=\frac{1+2\alpha\eta_L\varnothing_f}{1-\eta_L\varnothing_f} \tag{2}$$

$$\frac{E_{22}}{E_m}=\frac{1+2\eta_T\varnothing_f}{1-\eta_T\varnothing_f} \tag{3}$$

$$\frac{E_r}{E_m}=\frac{3}{8}\left[\frac{1+2\alpha\eta_L\varnothing_f}{1-\eta_L\varnothing_f}\right]+\frac{5}{8}\left[\frac{1+2\eta_T\varnothing_f}{1-\eta_T\varnothing_f}\right] \tag{4}$$

where $\eta_T=\left(E_f/E_m-1\right)/\left(E_f/E_m+2\right)$, and $\eta_L=\left(E_f/E_m-1\right)/\left(E_f/E_m+2\alpha\right)$. E, E_m, and E_f are the elastic modulus of the composites, matrix, and filler, respectively. E_f is set as 200 GPa[24,41] in this case. $\varnothing_f$ is the volume fraction of filler. α is the aspect ratio of the filler, which is set as 150 according to the MWCNT dimensional parameters.

The effect of the addition of MWCNTs on stress at break (σ_b) and strain at break ε_b are shown in Figure 7(b), from which one can see the MWCNTs exhibit a clear negative effect on the σ_b and ε_b of all the composites. The σ_b and ε_b of the composites with only 2 wt % MWCNTs decreases by 39% and 92%, respectively, before levelling off in this case (Table III). This can be mainly attributed to the presence of nanotube agglomerates in the HDPE/MWCNT composites, because these agglomerates can work as initiation sites for the generation and extension of cracks.[37,42]

The tensile properties of the blown films of pure HDPE and HDPE/MWCNT composite containing 4 wt % MWCNTs were also investigated at different BURs. Figure 8 shows the tensile strain–stress curves of the samples at BURs of 2 and 3, in which each curve is selected from five repeated tests for data representation. The apparent fluctuations in the initial stages of the stress–strain curves are due to the transition of the crosshead speed from 5 to 50 mm/min. The Young's modulus, stress at break and strain at break of the blown films with increasing BURs are shown in Figure 9, and compared with the results of compression molded samples. It can be observed in Figure 8 that the blown film of pure HDPE exhibits a higher tensile strength in the MD than TD at a BUR of 2, while this phenomenon is reversed at a BUR of 3. This may be attributed to some of the lamellae stacked perpendicular to the MD changing their orientation to the TD with increasing BURs.[19,21] The tensile stress for the HDPE/MWCNT composite films is clearly higher than that for the pure HDPE films at the same strain due to the reinforcing effect of the MWCNTs, while the elongation of the composite films decreases markedly compared with the pure HDPE. In addition, the higher tensile strength always occurs in the MD for the blown films of the composite, indicating that more MWCNTs are probably aligned along the MD even at a BUR of 3. This may be due to less potential for molecular relaxation in the MD due to more rapid cooling (better heat transfer due to MWCNTs).[43]

It can be seen in Figure 9(a) that the modulus of the blown films of pure HDPE is increased by 6∼25% on average in the MD and TD at different BURs compared to the compression molded HDPE sample, due to the orientation of polymer chains. An evident anisotropy in modulus can be observed for the composite with 4 wt % MWCNTs at a BUR of 2, where the modulus in the MD is 51% higher than that in the TD. At this BUR, the clearly higher modulus in the MD can be attributed to more MWCNTs being oriented along the MD. Then the difference in modulus in the MD and TD is weakened gradually, because some nanotubes may be reoriented along TD with increasing BURs [Figure 5(d–e)]. At BURs of 2.5 and 3, the modulus of the composite thin films is not improved

Table III. Changes in the Tensile Properties of the Compression Molded Sheets and Blown Films of HDPE/MWCNT Composites Compared to the Pure HDPE

Sample	ΔE (%)	$\Delta\sigma_b$ (%)	$\Delta\varepsilon_b$ (%)
CNT2-CM	+42.0	−38.5	−92.3
CNT4-CM	+111.6	−40.5	−94.8
CNT8-CM	+163.4	−34.6	−97.8
CNT4-BUR2-MD	+123.9	−2.6	−53.0
CNT4-BUR2-TD	+52.4	−19.2	−73.7
CNT4-BUR2.5-MD	+116.6	−1.4	−46.6
CNT4-BUR2.5-TD	+74.5	−20.0	−60.3
CNT4-BUR3-MD	+114.1	+28.8	−34.5
CNT4-BUR3-TD	+80.7	−7.1	−55.3

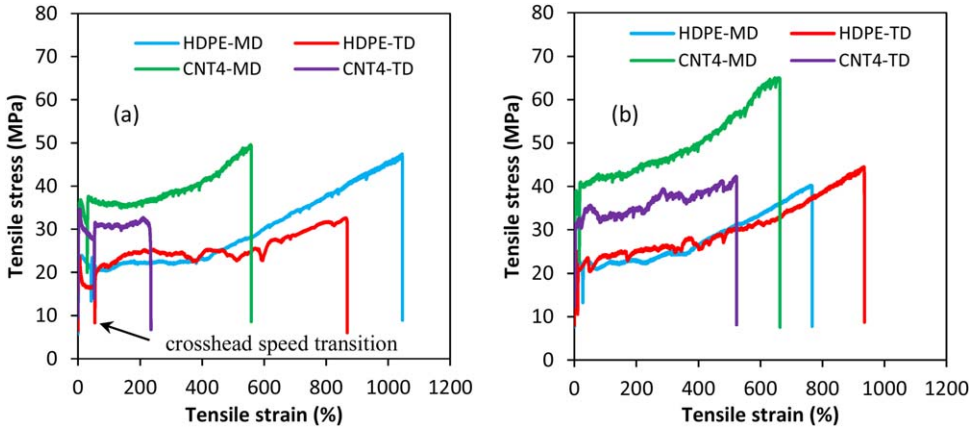

Figure 8. Tensile strain–stress curves of the blown films of pure HDPE and HDPE/MWCNT composite containing 4 wt % MWCNTs at BURs of 2 (a) and 3 (b). [Color figure can be viewed in the online issue, which is available at wileyonlinelibrary.com.]

significantly in both MD and TD relative to the compression molded sample. The predicted modulus in the MD (E_{11}) and TD (E_{22}) by a fully aligned Halpin-Tsai model (eqs. (2) and (3), respectively) shows large errors relative to the experimental values as a result of the biaxial orientation during blown film extrusion.[22] Biaxial orientation results in MWCNTs being aligned in the MD, in the TD and at orientations in between these. Therefore, it is reasonable that all the predicted values in the MD (CNT4-E_{11}) via the fully aligned Halpin-Tsai model are much higher than the experimental values (CNT4-MD), while all the predicted values in the TD (CNT-E_{22}) are much lower than the experimental values (CNT4-TD). The predicted modulus (E_r) by a randomly aligned Halpin-Tsai model (eq. (4)) is always between the experimental modulus in the MD and TD, and agrees very well with the experimental values at BURs of 2.5 and 3 due to the enhanced biaxial orientation [Figure 9(a)]. It can be observed in Figure 9(b,c) that the stress at break and strain at break of the blown films of HDPE/MWCNT composite increases steadily in the MD and TD with increasing BURs due to the breakup of MWCNT agglomerates. At a BUR of 3, the σ_b of the composite film increases by 239% and 154% in the MD and TD, respectively, and the ε_b increases significantly by 1054% and 828% in the MD and TD, respectively, compared to the compression molded composite sample. The ε_b of pure HDPE is not influenced substantially by blown film extrusion [Figure 9(c)], while the σ_b of all the blown films of pure HDPE increases by about 57% on average, which is mainly attributed to the enhanced orientation of polymer chains (the crystallinity of the blown films of pure HDPE is not increased, as shown in Table II).

The effect of the addition of 4 wt % MWCNTs on the tensile properties of blown films is shown in Table III. One can see that the inclusion of MWCNTs results in a significant enhancement in the Young's modulus of the blown films, especially in the MD. However, it may also lead to a decrease in the breaking strength of the blown films. With the inclusion of MWCNTs, similar effects on the tensile properties of blown films of TPU/MWCNT composites were also observed.[22] At a BUR of 3, the modulus and stress at break of the composite film increase by about 114% and 29%, respectively, in the MD, but the strain at break decreases by about 35% compared to the pure HDPE film (Table III).

Electrical Resistivity Testing

The electrical properties of the HDPE/MWCNT composites were characterized by measuring the volume resistivity of compression molded sheets and blown films at different BURs, as shown in Figure 10. The compression molded composite containing only 2 wt % MWCNTs exhibits a great decrease of 13 orders of magnitude in resistivity relative to the pure HDPE sheet. It indicates that many conductive pathways have been formed in the polymer matrix with the addition of 2 wt % MWCNTs. This composite (2 wt % MWCNTs) exhibits a lower resistivity ($\sim 3\times10^4$ Ω cm) compared to that ($\sim 1\times10^8$ Ω cm) obtained in Verge's study[44] of melt mixed composite with 3 wt % MWCNTs, in which the same HDPE matrix (HTA-108) and MWCNTs (NC7000) were used. The significant decrease in the resistivity of the composites may be attributed to the homogeneous dispersion of individual nanotubes and secondary nanotube agglomerates resulting from the effective melt mixing achieved in this work. The resistivity of compression molded composites further decreases at decreasing rates with the addition of more MWCNTs. At a MWCNT loading of 10 wt %, the compression molded composite exhibits a low resistivity of ~10 Ω cm as a result of the enhanced conductive networks.

The resistivity of the blown films of pure HDPE and the composites with 2 and 4 wt % MWCNTs was measured in the thickness direction using the high resistivity electrometer, and the resistivity of the blown films of composite with 8 wt % MWCNTs was measured in the MD and TD using the multimeter. As expected, it can be seen from Figure 10 that the resistivity of pure HDPE is barely influenced by blown film extrusion. However, the resistivity of the composite with 2 wt % MWCNTs increases by 10 orders of magnitude at a BUR of 2 before levelling off. It is likely that at this BUR the distance between the MWCNTs exceeds the critical maximum distance of 1.8 nm[45] for electron hopping. For the composite with 4 wt % MWCNTs, the resistivity of blown films increases steadily with increasing BURs, and it also increases by about 10 orders of magnitude when the BUR increases to 3. However, there is no significant

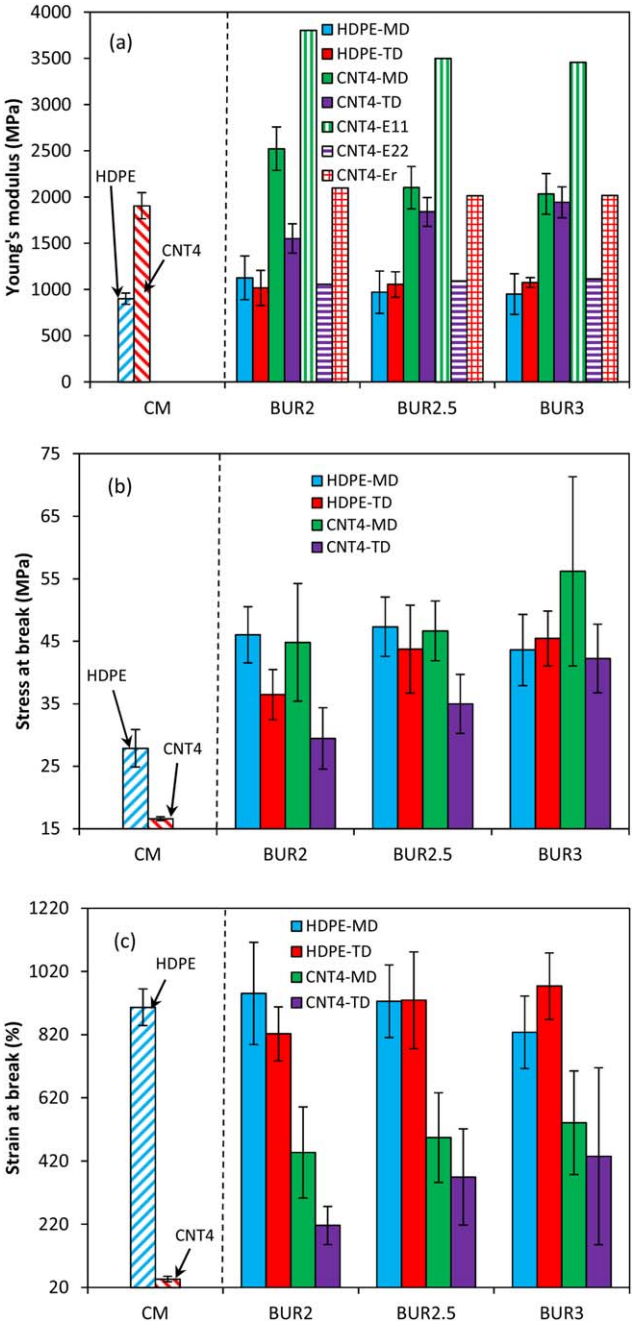

Figure 9. Young's modulus (a), stress at break (b), and strain at break (c) of the blown films of pure HDPE and HDPE/MWCNT (4 wt %) composite with increasing BURs. (In Figure 9(a), the modulus of matrix used for the calculation of CNT4-E_r is the average modulus of HDPE film in the MD and TD at each BUR). [Color figure can be viewed in the online issue, which is available at wileyonlinelibrary.com.]

increase in the resistivity of the composite containing 8 wt % MWCNTs after film blowing at increasing BURs. This implies that at this loading there is a sufficient density of nanotubes to form a robust conductive network in the matrix. It can be observed in the inset of Figure 10 that the resistivity of the composite film with 8 wt % MWCNTs is very close in the MD and TD with the resistivity in the MD being slightly lower than

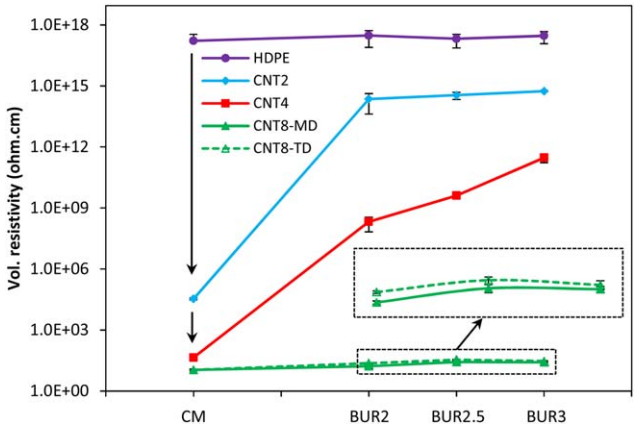

Figure 10. Changes in the volume resistivity of the blown films of HDPE/MWCNT composites with increasing BURs. [Color figure can be viewed in the online issue, which is available at wileyonlinelibrary.com.]

that in the TD probably due to relatively more MWCNTs aligned in the MD. In general, here the changes in the volume resistivity of the blown films of HDPE/MWCNT composites are similar to the changes in the volume resistivity of the biaxially stretched HDPE/MWCNT composites reported in author's previous work.[13]

The blown films of the composite containing 4 wt % MWCNTs with different BURs were annealed under different conditions in order to investigate the effect of annealing on the volume resistivity of the composite films. The detailed annealing parameters are presented in Table I. In order to simulate the crystallinity of the blown films of HDPE/MWCNT composites during the annealing process, DSC testing with combined isothermal and non-isothermal stages was conducted, as shown in the inset of Figure 11. It can be observed in the inset of Figure 11 that there is no melting peak present indicating no crystallites remaining in the sample even after a heating stage at 130°C for 5 min,

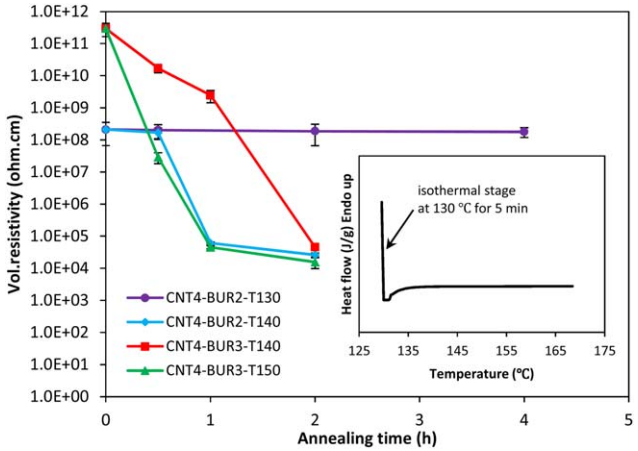

Figure 11. Changes in the volume resistivity of the blown films of HDPE/MWCNT composite with 4 wt % MWCNTs after annealing (Inset: DSC thermograms with combined isothermal and non-isothermal stages for assessing the crystallinity of the blown film containing 4 wt % MWCNTs after heating at 130°C for 5 min). [Color figure can be viewed in the online issue, which is available at wileyonlinelibrary.com.]

thus it is reasonable to assume that there are no crystallites remaining in the samples under all the annealing conditions. Furthermore, the residual crystallites should not be considered as a factor affecting the resistivity variation of samples during annealing.

The changes in the volume resistivity of the blown films of HDPE/MWCNT composite with 4 wt % MWCNTs after annealing are shown in Figure 11. It can be seen from Figure 11 that the resistivity of the composite film at a BUR of 2 is barely influenced by the annealing process at 130°C, but it decreases by 4 orders of magnitude after annealing at 140°C for 1 h. Similarly, the resistivity of composite films at a BUR of 3 decreases by 7 orders of magnitude after annealing at 140°C for 2 h or annealing at 150°C for 1 h. Figure 5(f) shows the relaxed MWCNTs in the blown film of composite with 4 wt % MWCNTs at a BUR of 3 after an annealing process at 140°C for 2 h. It is clear that a higher annealing temperature benefits the recovery of the conductive network of MWCNTs. This can be attributed to the decreased viscosity of the polymer matrix and increased mobility of nanotubes at a higher annealing temperature facilitating the reformation of local contacts between MWCNTs and reaggregation of MWCNTs.[46] One can suggest that composite thin films with a smaller BUR (less deformation) will require a shorter time to repair the conductive network during annealing. Some previous studies[33,46] have also found that the electrical properties of polymer/MWCNT composites after extensional deformation can be enhanced by annealing at an appropriate annealing temperature.

CONCLUSIONS

In this work, melt mixed HDPE/MWCNT nanocomposites with 2, 4, and 8 wt % MWCNTs were prepared using a twin-screw extruder and then processed by compression molding and blown film extrusion. During blown film extrusion, the pressure in the extruder barrel increases with increasing MWCNT content due to the increased viscosity of the melt. With the inclusion of MWCNTs, the circumferential thickness distribution of the blown films is more uniform. SEM results show that the MWCNTs are randomly oriented in the compression molded composites, while there are more MWCNTs aligned along the MD in the blown composite films. DSC results indicate that the crystallinity and crystallization temperature of the pure HDPE and HDPE/MWCNT composites are not substantially affected by blown film extrusion, while the melting temperature of all the blown films decreases by about 1∼2°C relative to the compression molded samples due to the decreased crystallite size resulting from the rapid cooling during film blowing. Tensile results show that the modulus of compression molded composites with 2, 4, and 8 wt % MWCNTs significantly increases by 42%, 112%, and 163%, respectively. An evident anisotropy in modulus can be observed for the composite with 4 wt % MWCNTs at a BUR of 2, where the modulus in the MD is 51% higher than that in the TD. Then the difference in modulus in the MD and TD is weakened gradually probably due to the reorientation of some MWCNTs along the TD with increasing BURs. The predicted modulus using a randomly aligned Halpin-Tsai model agrees very well with the experimental values at BURs of 2.5 and 3. The stress and strain at break of the composite films increases steadily with increasing BURs due to the breakup of MWCNT agglomerates. Volume resistivity testing indicates that blown film extrusion has a destructive effect on the conductive pathways of nanotubes in the polymer. The resistivity of the composite with 2 wt % MWCNTs increased by 10 orders of magnitude at a BUR of 2 before levelling off relative to the compression molded sample. However, there is no significant increase in the resistivity of the composite containing 8 wt % MWCNTs after film blowing at increasing BURs due to a sufficient density of nanotubes forming a robust conductive network. The conductive network in the blown films of HDPE/MWCNT composite with 4 wt % MWCNTs can be recovered partially after an appropriate annealing process. A higher annealing temperature facilitates the recovery of the conductive network of nanotubes. In addition, the composite films with a smaller BUR may require a shorter time to repair the conductive network during annealing. In this study, the blown films of HDPE/MWCNT composites with excellent mechanical properties and tailored electrical properties reveal potential applications in packaging of electronic components and aerospace and automotive industries for antistatic and electrostatic dissipation etc.

ACKNOWLEDGMENTS

The authors would like to thank Nanocyl S.A., Belgium for providing the MWCNTs and Dr. Paul Baine for his help in plasma etching. Dong Xiang gives his deep gratitude to CSC and QUB Overseas Scholarship for the financial support provided.

REFERENCES

1. Khan, S. U.; Pothnis, J. R.; Kim, J. K. *Compos. A* **2013**, *49*, 26.
2. Fei, G.; Tuinea-Bobe, C.; Li, D.; Li, G.; Whiteside, B.; Coates, P.; Xia, H. *RSC Adv.* **2013**, *3*, 24132.
3. Gomes, D.; Loos, M. R.; Wichmann, M. H.; de la Vega, A.; Schulte, K. *Compos. Sci. Technol.* **2009**, *69*, 220.
4. Wang, Q.; Dai, J.; Li, W.; Wei, Z.; Jiang, J. *Compos. Sci. Technol.* **2008**, *68*, 1644.
5. Villmow, T.; Pötschke, P.; Pegel, S.; Häussler, L.; Kretzschmar, B. *Polymer* **2008**, *49*, 3500.
6. McNally, T.; Pötschke, P.; Halley, P.; Murphy, M.; Martin, D.; Bell, S. E. J.; Brennan, G. P.; Bein, D.; Lemoine, P.; Quinn, J. P. *Polymer* **2005**, *46*, 8222.
7. McClory, C.; Pötschke, P.; McNally, T. *Macromol. Mater. Eng.* **2011**, *296*, 59.
8. McClory, C.; McNally, T.; Baxendale, M.; Pötschke, P.; Blau, W.; Ruether, M. *Eur. Polym. J.* **2010**, *46*, 854.
9. Russo, P.; Acierno, D.; Marletta, G.; Destri, G. L. *Eur. Polym. J.* **2013**, *49*, 3155.
10. Socher, R.; Krause, B.; Müller, M. T.; Boldt, R.; Pötschke, P. *Polymer* **2012**, *53*, 495.
11. Mayoral, B.; Lopes, J.; McNally, T. *Macromol. Mater. Eng.* **2014**, *299*, 609.

12. Mayoral, B.; Garrett, G.; McNally, T. *Macromol. Mater. Eng.* **2014**, *299*, 748.
13. Xiang, D.; Harkin-Jones, E.; Linton, D. *RSC Adv.* **2014**, *4*, 44130.
14. Prashantha, K.; Soulestin, J.; Lacrampe, M.; Krawczak, P.; Dupin, G.; Claes, M. *Compos. Sci. Technol.* **2009**, *69*, 1756.
15. Kasaliwal, G.; Göldel, A.; Pötschke, P. *J. Appl. Polym. Sci.* **2009**, *112*, 3494.
16. Yu, D. R.; Kim, G. H. *J. Appl. Polym. Sci.* **2012**, *124*, 2962.
17. Choong, G. Y. H.; Lew, C. Y.; Focatiis, D.; Antonio, D. S. *J. Appl. Polym. Sci.* **2015**, *132*, 42277.
18. Yu, G.; Li, X.; Lieber, C. M.; Cao, A. *J. Mater. Chem.* **2008**, *18*, 728.
19. Zhang, X.; Elkoun, S.; Ajji, A.; Huneault, M. *Polymer* **2004**, *45*, 217.
20. Ghaneh-Fard, A.; Carreau, P.; Lafleur, P. *Polym. Eng. Sci.* **2004**, *37*, 1148.
21. Fatahi, S.; Ajji, A.; Lafleur, P. G. *Polym. Eng. Sci.* **2007**, *47*, 1430.
22. Russo, P.; Lavorgna, M.; Piscitelli, F.; Acierno, D.; Di Maio, L. *Eur. Polym. J.* **2013**, *49*, 379.
23. Abu-Zurayk, R.; Harkin-Jones, E. *Polym. Eng. Sci.* **2012**, *52*, 2360.
24. Morcom, M.; Atkinson, K.; Simon, G. P. *Polymer* **2010**, *51*, 3540.
25. Wunderlich, B. Macromolecular Physics, Crystal Melting; Academic Press: New York, **1980**; Vol. *3*.
26. Abu-Zurayk, R.; Harkin-Jones, E.; McNally, T.; Menary, G.; Martin, P.; Armstrong, C.; McAfee, M. *Compos. Sci. Technol.* **2010**, *70*, 1353.
27. Abu-Zurayk, R.; Harkin-Jones, E.; McNally, T.; Menary, G.; Martin, P.; Armstrong, C. *Compos. Sci. Technol.* **2009**, *69*, 1644.
28. Shen, Y.; Harkin-Jones, E.; Hornsby, P.; McNally, T.; Abu-Zurayk, R. *Compos. Sci. Technol.* **2011**, *71*, 758.
29. Abdel-Goad, M.; Pötschke, P.; Zhou, D.; Mark, J. E.; Heinrich, G. *J. Macromol. Sci. Pure Appl. Chem.* **2007**, *44*, 591.
30. Xiang, D.; Harkin-Jones, E.; Linton, D. *RSC Adv.* **2015**, *5*, 47555.
31. Alig, I.; Skipa, T.; Engel, M.; Lellinger, D.; Pegel, S.; Pötschke, P. *Phys. Stat. Sol. (b)* **2007**, *244*, 4223.
32. Jiang, Z.; Chen, Y.; Liu, Z. *J. Polym. Res.* **2014**, *21*, 1.
33. Mayoral, B.; Hornsby, P. R.; McNally, T.; Schiller, T. L.; Jack, K.; Martin, D. *J. RSC Adv.* **2013**, *3*, 5162.
34. Shen, J.; Champagne, M. F.; Yang, Z.; Yu, Q.; Gendron, R.; Guo, S. *Compos. A* **2012**, *43*, 1448.
35. Haggenmueller, R.; Fischer, J. E. Winey, K. I. *Macromolecules* **2006**, *39*, 2964.
36. Yang, J.; Wang, K.; Deng, H.; Chen, F.; Fu, Q. *Polymer* **2010**, *51*, 774.
37. Pöllänen, M.; Pirinen, S.; Suvanto, M.; Pakkanen, T. T. *Compos. Sci. Technol.* **2011**, *71*, 1353.
38. Coleman, J. N.; Khan, U.; Blau, W. J.; Gun'ko, Y. K. *Carbon* **2006**, *44*, 1624.
39. Affdl, J.; Kardos, J. *Polym. Eng. Sci.* **1976**, *16*, 344.
40. McNally, T.; Boyd, P.; McClory, C.; Bien, D.; Moore, I.; Millar, B.; Davidson, J.; Carroll, T. *J. Appl. Polym. Sci.* **2008**, *107*, 2015.
41. Jiang, Z.; Hornsby, P.; McCool, R.; Murphy, A. *J. Appl. Polym. Sci.* **2011**, *123*, 2676.
42. Ajayan, P. M.; Schadler, L. S.; Braun, P. V. Nanocomposite Science and Technology; Wiley-Vch: Weinheim, Germany, **2006**.
43. Han, Z.; Fina, A. *Prog. Polym. Sci.* **2011**, *36*, 914.
44. Verge, P.; Benali, S.; Bonnaud, L.; Minoia, A.; Mainil, M.; Lazzaroni, R.; Dubois, P. *Eur. Polym. J.* **2012**, *48*, 677.
45. Li, C.; Thostenson, E. T.; Chou, T. W. *Appl. Phys. Lett.* **2007**, *91*, 223114.
46. Zhang, S.; Lin, L.; Deng, H.; Gao, X.; Bilotti, E.; Peijs, T.; Zhang, Q.; Fu, Q. *Colloid Polym. Sci.* **2012**, *290*, 1393.